Design of a Serial-Parallel Robot with Piezo Actuators for Micro and Nano Manipulations

D. Chakarov, K. Kostadinov, T. Tiankov, M. Cveov
Institute of Mechanics, BAS, Acad. G. Bonchev Str., bl. 4, 1113, Sofia, Bulgaria
mit@imbm.bas.bg, kostadinov@imbm.bas.bg, tihomir@imbm.bas.bg

Abstract.
In this paper a piezo actuated micro robot is considered with a serial-parallel structure including elastic joints. A CAD model and principal components of the robot system are presented in the paper. A kinematics model of a serial-parallel structure is derived here. A pseudo rigid body approach is used, where elastic joints are modelled as revolute joints. An analysis of workspace and an evaluation of the inner forces by preliminary tension of the robot are carried out using this approach. Secondly, CAD - based finite element calculation are presented in order to estimate the values of mechanical parameters. The stiffness of basic components of the robot structure is evaluated using this technique.

Keywords: micro, nano, robot, piezo actuator, compliant joint, cell injection.

Introduction.
Micro and nano robots have emerged as an important technological advancement in the past twenty-five years. The significance of this advancement is highlighted in many applications where positioning of components within micrometer or nano meter accuracy is required. Micro and nano robots are mostly used in biological and microelectronics research, cellular technology, chemistry and investigation of thin films, in atomic force microscopes and scanning tunnelling microscopes. For instance, the positioning of samples in a scanning - electron microscopes, the alignment of fibre-optics and lasers, the positioning of wafers in micro-lithography, the manipulation of cells in micro-biology, the manipulation of micro-scale components in micro-assembly and disk drive micro actuation [1], [2], [3].
In order to obtain the required sub micron accuracy, the body of these micromanipulators are constituted of a high-precision mechanical structure which is free from backlash, friction and hysteresis. The body should also have a high structural frequency and be both rigid and compact. The arrangement in series of segments of manipulator body produces an accumulation and an amplification of errors. Another solution aimed towards increasing the stiffness of the structure without increasing its mass is the utilization of parallel structures [1].
As well known, parallel kinematic mechanisms possess inherent advantages over conventional serial manipulators, such as high rigidity, high load capacity, high velocity, and high precision, etc. However, as for any mechanical systems composed of conventional joints, traditional parallel manipulators suffer from errors due to backlash, hysteresis, and manufacturing errors in the joints. Hence, it is a major challenge to achieve ultrahigh precision with conventional joints.
On the other hand, compliant mechanisms, i.e., flexure based mechanisms can be employed into parallel mechanisms for high precision applications [4], [5] because compliant mechanisms exhibit many advantages in terms of vacuum compatibility, no backlash property, no nonlinear friction, simple structure and easy to manufacture.
Compliant mechanisms generate their motions through elastic deformation. These mechanisms use flexure hinges to replace the joints in a rigid-link mechanisms, thus avoiding the use of moving and sliding joints. The problems related to wear; backlash, friction and need for lubrication can thus be eliminated.
Many actuation principles have been applied to drive the compliant mechanism in a micro and nano robots. Piezoelectric actuators, electrostatic, electromagnetic and shape memory alloy actuators have been utilised to provide fine motions to the micro and nano robots. Since their resolution is dependent solely on the quality of applied voltage signal, piezoelectric actuators are commonly used to provide fine resolution of input displacements in subnanometer range [3], [6]. The use of a joint less compliant mechanism to provide motion transfer means that the position accuracy of such micro-motion mechanisms depends only on the accuracy of the piezoelectric actuator and the position sensor. Therefore, the compliant mechanism based micro and a nano robot is capable of achieving micrometer or even nanometer positioning resolution.
The objective of the work presented in this paper is to derive the design of a new 3-DOF spatial micromanipulator with a workspace covering the space range of about 180 μm x180μm x μm60 μm

and the resolution of several nanometers capable of performing automatic cell injection. A novel serial-parallel manipulator is designed to achieve such purposes.

Description and development of the micromanipulator.

The robot system includes a macromanipulator and a local micromanipulator. The macromanipulator is scheduled to insert the micromanipulator with the injection pipette in hand in the working zone. Here the biological cells on the range of 10-30 [μm] are preliminary positioned in a matrix. The aim of the micromanipulator is to orientate and to position the pipette according to the cells, as well as to perform the injection motions. The micro manipulator possesses a serial-parallel structure [7] as shown in the simulation if Fig.1. The manipulator body 1 is linked with the base 0 by means of an elastic joint J_3 forming a serial chain. Actuators A_1 and A_2 are located perpendicularly to the body 1, and they are linked with the base 0 by means of elastic joints J_1 and J_2, thus forming parallel chains. The actuators are fixed to the body 1 via spherical joints. Parallel structure comprising actuators A_1 and A_2 perform orientation motions, while the actuator A_3 performs injection through the pipette 2 attached to it.
Piezoelectric stack actuators are chosen, hereafter called piezoactuators, for their smooth motion, high accuracy, and fast response. The drawback of piezoelectric actuators is their limited stroke. PZT actuators are chosen, which possess the stoke of 30 μm. An enlarging the motion device is attached to the piezoactuator performing the injection motions.

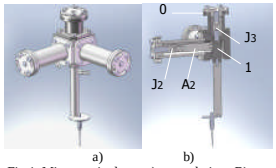

a) b)

Fig.1. Micromanipulator: a) general view; B) cross section

The spherical joints comprise contact joints including metal spheres by manufacturing attached to the top of the piezoactuators, which are implemented in cone sockets of the basic body 1. The joints J_1, J_2 and J_3 are recognized as double notched elastic beam joints. These joints possess a series of advantages as compared with the contact ones, as free from backlash, friction, and hysteresis. These joints, as well, allow by means of a preliminary deformation to achieve pretension of the piezoaductors. The joint geometry presented in Fig. 3 is accomplished by the help of electro-discharge machining. This geometry allows to be achieved the desired low stiffness in two transverse mutually perpendicular directions of bending and high stiffness in axial non-motional direction. The joint bending range is mechanically limited by the width of the slot at the electro-discharge machining, in order to be avoided increasing of the admissible yield strength σ of the material and a joint damage. Joints with variable stiffness are produced by means of variation of the width Δ of the most bending loaded area, as is shown further on.

Pseudo rigid body (PRB) modelling of the micro manipulator.

The pseudo-rigid-body-model is commonly used [2], [5], and [6] in order to predict the displacements of compliant mechanisms with elastic joints. As a rule it models an elastic joint as a revolute joint with a torsion spring attached to it. The pseudo-rigid-body method is effective and it simplifies the model of compliant mechanisms. Universal joint with torsion stiffness, PRB model of the manipulator was developed with the mechanism topology identified and each 2 DoF elastic joints replaced by a 2 DoF as shown in Fig. 2.

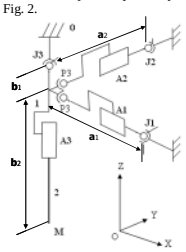

Fig.2. Kinematical chain of micro-manipulator with 3 DoF.

Base 0, manipulator body 1, actuator A_3 with working tool 2 and end- effector M form a serial chain. The body 1 is linked with the base 0 by means of 2 DoF universal joints J_3. Actuators A_1 and A_2 are linked with the base 0 by means of 2 DoF universal joints J_1 and J_2, thus forming parallel chains. The actuators are fixed to the body 1 via 3 DoF spherical joints P3. Actuators A_1 and A_2 are modelled as 1 DoF prismatic joints. According this model with rigid biddies and kinematic joints, the number DoF of the structure is h=3.

According this model generalized parameters are accepted to be the parameters of the relative motions in all joints - elastic and non-elastic of the structure [8], presented by vectors where

$$\mathbf{q} = [q_1, q_2, q_3]^T \quad (1)$$

is a vector of the generalized coordinates in the joints of the main serial chain with 3 DoF and

$$\mathbf{w} = [w_{11}, w_{12}, w_{21}, w_{22}]^T, \quad (2)$$

is a vector of coordinates in the passive universal joints of the parallel chains, and

$$\mathbf{l} = [l_1, l_2, l_3]^T, \quad (3)$$

is a vector of coordinates in the motor linear joints.
Let the linear coordinates of the end effector M are denoted as

$$\mathbf{X} = [X_1, X_2, X_3]^T \quad (4)$$

The relation between the parameters of the basic serial chain (1) and the parameters of the end effector (4) is known as a direct problem of the kinematics of the serial chain $\mathbf{X} = \Psi(\mathbf{q})$. This problem on the level of velocities is presented by the equations

$$\dot{\mathbf{X}} = \mathbf{J}\dot{\mathbf{q}} \quad (5)$$

where $\mathbf{J} = [\partial X/\partial q]$ is the (3 x 3) matrix of Jacoby.
In the parallel structure each closed loop implies the appearance of a connection between the generalized parameters (1),(2),(3). These connections are expressed by 6 scalar functions for the structure including 2 parallel loops: $\Psi_i(\mathbf{q}, \mathbf{w}, \mathbf{l}) = 0, i = 1,...,6$. The differentiation of above equations gives the relation

$$\mathbf{H}_q \frac{d\mathbf{q}}{dt} + \mathbf{H}_w \frac{\partial \mathbf{w}}{\partial \mathbf{q}} \frac{\partial \mathbf{q}}{\partial t} + \mathbf{H}_l \frac{\partial \mathbf{l}}{\partial \mathbf{q}} \frac{\partial \mathbf{q}}{\partial t} = \mathbf{0} \quad (6)$$

Using above matrix of partial derivations $\mathbf{W} = \partial \mathbf{w}/\partial \mathbf{q}$ and $\mathbf{L} = \partial \mathbf{l}/\partial \mathbf{q}$ with size (4 x 3) and (3 x 3) we have the relations between generalized velocities:

$$\dot{\mathbf{w}} = \mathbf{W}\dot{\mathbf{q}} \quad (7)$$

$$\dot{\mathbf{l}} = \mathbf{L}\dot{\mathbf{q}} \quad (8)$$

As the number of parameters (3) is equal to the DoF h = 3, these parameters can be selected as independent parameters. In equation (8) we have inverse relation:

$$\dot{\mathbf{q}} = \mathbf{L}^{-1}\dot{\mathbf{l}} \quad (9)$$

Equations (5) and (9) allow determining the velocities of end-effector, while equations (7) and (9) - the velocities of passive joints, as a function of the velocities of the linear actuator joins $\dot{\mathbf{l}}$:

$$\dot{\mathbf{X}} = \mathbf{J}\mathbf{L}^{-1}\dot{\mathbf{l}} \quad \text{and} \quad (10)$$

$$\dot{\mathbf{w}} = \mathbf{W}\mathbf{L}^{-1}\dot{\mathbf{l}} \quad (11)$$

The displacements of the piezo-actuators are small as compared to the link lengths. Therefore, the micromanipulator is almost configurationally invariant and its matrix of partial derivations **J, L** and **W** are assumed to be constants [2]. The equations (10), (11) give the relations between small displacements of microactuators Δl, small displacements of the end-effector ΔX and small displacements in passive joints $\Delta \mathbf{w}$:

$$\Delta \mathbf{X} = \mathbf{J}\mathbf{L}^{-1}\Delta \mathbf{l} \quad \text{and} \quad (12)$$

$$\Delta \mathbf{w} = \mathbf{W}\mathbf{L}^{-1}\Delta \mathbf{l} \quad (13)$$

In order to eliminate the backlash and to improve the performance of the piezo-actuators, a preliminary tensioning of the mechanical micromanipulation system is necessary. The following two approaches [8] can be used for tensioning of the manipulator:- deflection from the initial manipulator state by h driving joints motion introduced in the assembly; - preliminary tensioning of the separate elastic joints with number j, $(j \geq h)$.
According the first approach the tensioning can be achieved by means of an assembly deflection $\delta \mathbf{l}$ in the driving joints, which leads to deflection in all the system joints according to (9), (11) and deflection of the end-effector according to (10) defined by the equations:

$$\delta \mathbf{q} = \mathbf{L}^{-1}\delta \mathbf{l} \quad (14)$$

$$\delta \mathbf{w} = \mathbf{W}\delta \mathbf{q} = \mathbf{W}\mathbf{L}^{-1}\delta \mathbf{l} \quad (15)$$

$$\delta \mathbf{X} = \mathbf{J}\delta \mathbf{q} = \mathbf{J}\mathbf{L}^{-1}\delta \mathbf{l} \quad (16)$$

These deflections lead to elastic joints forces defined by the equations:

$$\mathbf{F}_q = \mathbf{k}_q \delta \mathbf{q} = \mathbf{k}_q \mathbf{L}^{-1}\delta \mathbf{l} \quad (17)$$

$$\mathbf{F}_w = \mathbf{k}_w \delta \mathbf{w} = \mathbf{k}_w \mathbf{W}\mathbf{L}^{-1}\delta \mathbf{l} \quad (18)$$

where $\mathbf{k}_q$ are angular stiffness matrices of the passive joints of the basic serial chain and $\mathbf{k}_w$ are angular stiffness matrices of the driving chains, respectively. The tensioned elastic system is in a static equilibrium [8] and allows definition of the forces of the driving joints $\mathbf{F}_l$ as a function of the forces $\mathbf{F}_q$, $\mathbf{F}_w$ in passive elastic joints.

$$\mathbf{F}_l = -\mathbf{L}^{-T}[\mathbf{F}_q + \mathbf{W}^T \mathbf{F}_w] \quad (19)$$

Numerical experimentation and CAD based FEA techniques for stiffness and inner force estimation.

The main dimensions of the manipulator are $a_1=a_2=0.073$[m], $b_1=0.030$[m], $b_2=0.180$[m] as shown in Fig.3. Piezo actuators used have parameters specified in Table 1.

Table 1. Parameters of the actuators used.

Actuator	Travel [μm]	Resolution [nm]	Axial stiffness [N/μm]	Push/pull force capacity [N]	Torque limit [N/m]
A_1, A_2	30	0.6	27	1000/50	0.35
A_3	60	1.2	15	1000/50	0.35

We can easily derive the matrix of partial derivations **J, L** and **W, s**ince the manipulator under consideration is assembled with a special rectangle configuration, shown below**:**

$$\mathbf{J} = \begin{bmatrix} 0 & -b_2 & 0 \\ b_2 & 0 & 0 \\ 0 & 0 & 1 \end{bmatrix} = \begin{bmatrix} 0 & -0.180 & 0 \\ 0.180 & 0 & 0 \\ 0 & 0 & 1 \end{bmatrix} \quad (20)$$

$$\mathbf{L} = \begin{bmatrix} 0 & -b_1 & 0 \\ b_1 & 0 & 0 \\ 0 & 0 & 1 \end{bmatrix} = \begin{bmatrix} 0 & -0.030 & 0 \\ 0.030 & 0 & 0 \\ 0 & 0 & 1 \end{bmatrix} \quad (21)$$

$$\mathbf{W} = \begin{bmatrix} b_1/a_1 & 0 & 0 \\ 0 & 0 & 0 \\ 0 & b_1/a_2 & 0 \\ 0 & 0 & 0 \end{bmatrix} = \begin{bmatrix} 0.411 & 0 & 0 \\ 0 & 0 & 0 \\ 0 & 0.411 & 0 \\ 0 & 0 & 0 \end{bmatrix} \quad (22)$$

The calculation of the characteristic components using the matrix equalities (12), (13), (14), (15), (16), (19) is very easy and efficient with such a simple constant matrixes.

Equation (12) presents the manipulator transmissibility function

$$\mathbf{JL^{-1}} = \begin{bmatrix} 6 & 0 & 0 \\ 0 & 6 & 0 \\ 0 & 0 & 1 \end{bmatrix} \quad (23)$$

according to which at admissible micro displacements of the actuators presented by the vector $\mathbf{\Delta l = [30;30;60]^T 10^{-6}[m]}$ the admissible micro displacements of the end-effector are defined $\mathbf{\Delta X = [180;180;60]^T 10^{-6}[m]}$, which form the workspace range of the micromanipulator. The displacements in the passive joints $\mathbf{\Delta w}$ at the micro displacements of the actuators according (13) are less than those obtained by means of tensioning of the actuators and are going to be assessed further on. The tensioning of manipulator by means of deflection from the initial state is achieved by means of a deflection of the driving joints J_1, J_2 introduced in the assembly:

$$\mathbf{\delta l = [-260, -260, 0]^T 10^{-6}\,[m]} \quad (24)$$

in the two driving joints of the parallel structure. The resulting deflection in the elastic joints according to (14), (15) and the deflection of the end-effector according to (16) are:

$$\mathbf{\delta q = [-8.666;8.666;0]^T 10^{-3}}[\text{rad}] \quad (25)$$

$$\mathbf{\delta w = [3.562;0;-3.562;0]^T 10^{-3}}[\text{rad}] \quad (26)$$

$$\mathbf{\delta X = [-1.560;-1.560;0]^{-T} 10^{-3}}\ [\text{m}] \quad (27)$$

Deflections from the initial state (24) are selected in such a way, that the deviations in the elastic joints (25) and (26) to be less than one admissible value $\mathbf{\sigma = 8.726\ 10^{-3}\ [rad] = 0.5^0}$.

The suitable choice of the desired stiffness in the elastic joints $\mathbf{k_q}$, $\mathbf{k_w}$ defines the value of the internal forces and torques in the manipulator. The torque limit of the actuators according to Table 1 can be accepted as an admissible value of the torques at tensioning of the elastic joints $\mathbf{F^1_w = [0.35;0.35;0.35;0.35]^T}$ [Nm]. The value of the torques $\mathbf{Fw}$ in the elastic joints J_1, J_2 must be less than the admissible $\mathbf{F^1w}$ that is the reason to be selected commercial elastic joints with values of the angular coordinates $\mathbf{k_w}$ = **diag[40;40;40;40] [Nm/rad],** for which reason at tensioning (24), the torques (18) possess values

$$\mathbf{F_w = [0.14;0;-0.14;0]^T\ [Nm].} \quad (28)$$

Forces in the driving joints (29) which tension axially the aductors A_1, A_2 are defined basically of the stiffness of the elastic joint $\mathbf{J_3}$**.** The angular stiffness of the joint $\mathbf{J_3}$ must be within the range of **169 – 338 [Nm/rad]** if the value of both forces is selected to be 5%-10% from the push force capacity of the actuators used (Tabl.1) or $\mathbf{50[N] \le |F_{Ri}| \le 100\ [N],\ i=1,2,}$ according to equation (19).

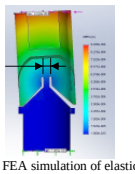

Fig.3. FEA simulation of elastic joint.

The elastic force is designed as double notched elastic beam joint. The joint geometry presented in Fig. 3 allows the desired angular stiffness to be achieved by means of variation of the width Δ of the most bending loaded area. An assessment of the realized stiffness is performed by means of using of FEA-based technique [6], [9] applied for the elastic joint as a separate element.

The stiffness matrix $\mathbf{k_q}$ is evaluated according to this technique from several numerical experiments, each of which produces the angular deflections (φ) corresponding to the applied torque (M). The angular stiffness matrix is three dimensional, symmetrical

matrix. It is assumed that the stiffness matrix is a diagonal one since the investigated object implies a simple geometry (a cylindrical bar) and thus each FEA experiment returns just one component of the matrix $\mathbf{k}_\eta$

The joint geometry and the FEA modelling are performed using the computer code SOLID WORKS CAD system. The selected material of elastic joint is titanium alloy (Ti-6Al-4V) with Young's modulus E = 104.8 [GPa] and Yield strength σ=1.05 [GPa]. The loading is applied in one single point in the modelling at the bar end which bar is clamped at the other end (please refer to Fig. 3. The following loadings is selected $\mathbf{M_x = M_y = (0.015x100) =1.5\ [Nm], Mz=2\ [Nm].}$ These loadings are applied in series and for each case the deflections are calculated from the reference point.

The deflections are computed several times in order to improve the precision [9] in different nodes located in the neighbourhood of reference point and the average value is adopted. One diagonal component of the stiffness matrix **K** is calculated at each experiment. The experiments are carried out for variable width Δ of the most bending loaded area. The results are presented in Table 2.

Table 2.

	K_{11} **[Nm/rad]**	K_{22} **[Nm/rad]**	K_{33} **[Nm/rad]**
Δ_1=0.0010[m]	34.09	34.09	183
Δ_2=0.0012[m]	49.07	49.07	225
Δ_3=0.0017[m]	114.73	114.73	329
Δ_4=0.0020[m]	172.41	172.41	363
Δ_5=0.0022[m]	196.16	196.16	414
Δ_5=0.0025[m]	271.24	271.24	432

The tensioning actuators forces are $\mathbf{F_1 = [58.57;58.57;0]^T\ [N]}$, if an elastic joint is selected with $\mathbf{\Delta_5=0.0022\ [m]}$ and angular stiffness $\mathbf{k_\eta}$ = **diag[196.16; 196.16; 414] [Nm/rad]** according to (17), the elastic joint torques J_3 are $\mathbf{F_q = [1.70;1.70;0]^T\ [Nm]}$ and according to (19), (28) , which is 6% from the push force capacity of the actuators. An elastic joint is manufactured possessing these parameters, which is mounted and the mechanical construction of the manipulator is tensioned to the cited above values. The robot with mechanical construction preliminary tensioned achieves minimal displacement obtained experimentally 30[nm].

Conclusion.

Piezo actuated micromanipulators with serial-parallel structure including elastic joints are the subject of this paper. The design of a new 3-DOF spatial micromanipulator with a workspace covering the space range of about 180 x180x 60 [μm] and the resolution of several nanometers capable of performing automatic cell injection is presented in the paper.

A CAD model and principal components of the robot system are shown in the paper. A kinematics model of a serial-parallel structure is build here. A pseudo rigid body approach is used, where elastic joints are modelled as revolute joints. Using this approach numerical experimentation and an analysis of workspace is carried out. In order to eliminate backlashes and to improve the performance of the piezo-actuators an evaluation of the inner forces by preliminary tension of the robot is obtained. Thus, the maximal values of the tensioning forces are achieved using appropriate elastic joints. In the paper, CAD - based finite element analysis (FEA) techniques are presented in order to estimate the stiffness values of the elastic joints.

Elastic joints are manufactured possessing the designed parameters by means of which the manipulator mechanical construction is tensioned to the calculated parameter values. Experiments and tests are under consideration for successful cell injection.

ACKNOWLEDGEMENTS:

This work was funded partially by the European Commission through the FP6 Integrated Project HYDROMEL with contract No. FP6 NMP2-CT-2006-026622, and by the National Science Foundation under the project "SpeSy-MiNT"/2009, to which the authors are expressing their acknowledgements.

References

[1] E. Pernette, S. Henein, I. Magnani and R. Clavel, Robotica, vol.15, (1997), pp.417-420.
[2] W. Zhang, J., Zou, L., Watson, W., Zhao, *Journal of Robotic Systems 19(2)*. (2002), 63–72.
[3] R. Kasper, M.Al-Wahab, 9th International Conference on New Actuators, ACTUATOR 2004, Bremen, Germany, (2004), 68-71.
[4] H. Pham, I.Chen, Precision. Engineering 29, (2005), 467–478.
[5] Y. K. Yong, Tien-Fu Lu, Mechanism and Machine Theory 43, (2008), 347-363.
[6] Y. Li and Q.Xu, IEEE/ASME Int. Conf. on Adv. Intelligent Mechatronics, Monterey, USA, 24-25 July, (2005), 93-98.
[7] K. Kostadinov, D. Chakarov, T. Tiankov, Fl. Ionescu, BG Patent, Reg. No 110432/28.07.2009.
[8] D. Chakarov, K. Kostadinov, T. Tiankov, Int. Conf. on Informatics in Control, Automation and Robotics, Milan, Italy, 2-5 July, Vol.2, (2009), 135-140.
[9] A. Pashkevich, A. Klimchik, D. Chablat, Ph. Wenger, 42 CIRP Conference on Manufacturing Systems, Grenoble, 3 - 5 Jun, (2009), 1-8.